NJC

Accepted Manuscript

This is an *Accepted Manuscript*, which has been through the Royal Society of Chemistry peer review process and has been accepted for publication.

Accepted Manuscripts are published online shortly after acceptance, before technical editing, formatting and proof reading. Using this free service, authors can make their results available to the community, in citable form, before we publish the edited article. We will replace this *Accepted Manuscript* with the edited and formatted *Advance Article* as soon as it is available.

You can find more information about *Accepted Manuscripts* in the Information for Authors.

Please note that technical editing may introduce minor changes to the text and/or graphics, which may alter content. The journal's standard Terms & Conditions and the Ethical guidelines still apply. In no event shall the Royal Society of Chemistry be held responsible for any errors or omissions in this *Accepted Manuscript* or any consequences arising from the use of any information it contains.

ROYAL SOCIETY OF CHEMISTRY

www.rsc.org/njc

Electrospun nitrogen and carbon co-doped porous TiO_2 nanofibers with high visible light photocatalytic activity

Xinping Liu[1,2], Yanying Chen[1,3], Changlin Cao[2,3], Jing Xu[1, 3], Qingrong Qian[1, 3*], Yongjin Luo[1,3], Hun Xue[1,3], Liren Xiao[2], Yuming Chen [1, 3], Qinghua Chen[1, 3*]

[1] College of Environmental Science and Engineering, [2] College of Materials Science and Engineering, Fujian Normal University, Fuzhou 350007, China

[3] Fujian Key Laboratory of Pollution Control & Resource Reuse, Fuzhou 350007, China

Abstract: Nitrogen and carbon co-doped porous TiO_2 nanofibers (NCPTNs) were exploited by a combination of electrospinning and controlled calcination technologies. Polyvinyl pyrrolidone (PVP) was employed both as a template and as a nitrogen and carbon resource. It is clear that the prepared NCPTNs exhibit high absorption in the visible light region, suggesting that the co-doping of nitrogen and carbon onto TiO_2 not only leads to a shift of the absorption edge to lower energy by inducing new band levels, but also creates large amounts of single-electron-trapped oxygen vacancy. Besides, the porous structure and high surface area provide large active points for the photodecomposition reaction of methylene blue. Moreover, The NCPTN obtained at 5 wt% urea shows the highest photocatalytic activity for methylene blue decomposition under the visible light irradiation.

Keywords: electrospinning, nitrogen and carbon co-dopping, TiO_2 nanofibers, photocatalytic activity, visible-light irradiation

1. Introduction

Photocatalytic semiconductor-based treatment is a promising green technology for the decomposition of toxic organic compounds in environment.[1,2] Titanium dioxide (TiO_2) has been considered as one of the most popular oxide semiconductors

* Corresponding authors. Tel. & Fax: +86-591 8346 5158
qrqian@fjnu.edu.cn (Q. Qian), cqhuar@fjnu.edu.cn (Q. Chen)

due to its high chemical stability and excellent photocatalytic mineralization of organic pollutants.[3,4,5] However, the poor solar light absorption capability of TiO_2 limits its applications. Codoping nonmetal elements in TiO_2 has been found to be an effective method to overcome the problem.[6,7] Tan *et al.* prepared the C-N co-doped TiO_2 films by using an organic-free sol-gel method, and proposed that the presence of Ti-O-C band and nitrogen surface species may lead to an increase of visible light photocatalytic activity.[8] Li *et al.* found that N-F co-doped TiO_2 nanomaterials had a higher visible-light photocatalytic activity than TiO_2 doped solely with nitrogen or fluorine.[9,10] Wu *et al*. reported their preparation of C-N co-doped TiO_2 films by using magnetron sputtering method.[11] Cong *et al*. synthesized the C-N-TiO_2 nanoparticles by a microemulsion-hydrothermal process and researched their structure and photocatalytic activity.[12] Sano *et al.* reported that the N,C-doped TiO_2 photocatalyst prepared via the calcination of Ti^{4+}-bipyridine complex, acting as the source of N and C, exhibited high photocatalytic activity for NO_x removal under both ultraviolet and visible-light illumination.[13] Daisuke *et al.* achieved deposition of $Ti(O,C,N)_2$ films co-doped with N and C using direct current reactive sputtering utilizing a Ti target in an $Ar/N_2/CO_2$ ambient, and confirmed N and C were at substitutional O sites.[14] Therefore, the visible light photoactivity of co-doped TiO_2 varies with preparation method and the precursors of nitrogen and carbon doping.

In recent years, electrospinning has been considered as a simple and versatile technique for producing one-dimensional (1D) TiO_2-based nanofiber photocatalysts.[15] Li *et al.* prepared mesoporous TiO_2 nanofibers by electrospinning in combination with calcination process. They found that the TiO_2 nanofibers obtained at 500℃ had the best photocatalytic activity.[16] Babu *et al.* fabricated N-TiO_2 rice grain-like structures using sol-gel and electrospinning methods followed by post-annealing of the composite nanofibers.[17] Many researches are focused on fabricating various morophologies of TiO_2, such as nanotube, tube-in-tube porous nanofibers,[18] mesoporous,[16] metal doped TiO_2, etc.[19] In these contributions, PVP is considered as a promising template for fabrication of the PVP/TiO_2 composite fibers. It is believed that the role of PVP is to increase the solution viscosity and thus to control the

viscoelastic behaviour for spinability. To obtain metal oxide nanofibres, the PVP should be removed from the resultant PVP/TiO_2 composite fibers after electrospinning. Therefore, the calcination should be often conducted at 500℃ for above 3 h.[20,21] As we know, PVP can be made a macroligand through the polar groups for stabilizing metallic nanocryatals with fibers due to its amphiphilic and nonionic structures [22,23]. Furthermore, PVP is thermally degraded, predominantly, by the release of the pyrrolidone side group and the subsequent decomposition of polyenic sequences in the presence of oxygen.[24] Pyrrolidone units can form strong coordinating bonds via amine-N and carbonyl-O donors, which bridge adjacent metal atoms on the nanoparticles surfaces. Borodko *et al.* believed that released pyrrolidone moieties near the metal surface are chemisorbed as bridging ligands.[25] Wu *et al.* suggested that the PVP could not decompose completely at temperatures less than 500℃ in the process of calcining PVP/SnO_2 nanofibers.[26] However, there has been no literature reporting the effects of N and O elements contained in PVP on the electronic structure, crystal structure and catalytic properties of TiO_2 synthesized by electrospinning and a calcinating process at 400℃.

In this paper, PVP was selected as a template to obtain the electrospun composite nanofibers precursor for preparing a novel N and C co-doped porous TiO_2 nanofibers (NCPTNs). PVP also plays a role of nitrogen and carbon resource for the in situ co-doping of N and C on the TiO_2 nanofibers. For the comparison, urea was also introduced as a nitrogen resource in the precursor. The photocatalytic property of the resultant NCPTNs was evaluated using methylene blue as a model toxic organic compound under visible light irradiation.

2. Experimental

2.1 Preparation

NCPTNs were prepared by a combination of electrospinning and calcination method. The electrospinning solutions were prepared by mixing 1.0 g PVP (M_w: 1300000, Aldrich), 1.5 mL $Ti(OiPr)_4$ (Aldrich) and an appropriate amount of urea in a mixture solvent of 20 mL ethanol and 3 mL acetic acid in a 100 mL Erlenmeyer flask.

The solution was stirred at room temperature for 2 h prior to the electrospinning. The spinneret used in the experiment consisted of a stainless-steel tube with a diameter of 0.6 mm. A high voltage of 17 kV was supplied at the spinneret by a direct-current power supply (DW-P503-4AC). The liquid was fed in at a rate of 0.5 mL/h with a syringe pump (WZS-50F6). The electrospun PVP/$Ti(OiPr)_4$/urea composite fibers were collected on a tin foil. All experiments were conducted at room temperature in air. The collected electrospun composite fibers were subsequently calcined in air at 400 ℃ for 1 h with heating rate of 5℃/min to obtain the NCPTNs. The samples obtained from different amounts of urea of 0, 1, 3, 5, 10 and 20 wt% were denoted as NCPTN-0, NCPTN-1, NCPTN-3, NCPTN-5, NCPTN-10 and NCPTN-20, respectively.

2.2 Characterization

The phase of the NCPTNs was determined on an X-ray diffraction analyzer (XRD, Philips, X'Pert Pro MPD) using graphite mono-chromized CuK_α radiation. The accelerating voltage and the applied current were 40 kV and 40 mA, respectively. The size and morphology of the NCPTNs were analyzed on a field emission scanning electron microscope (FESEM, JEOL, JSM-7500F), a transmission electron microscopy (TEM, JEOL JEM-2100F) with Energy-dispersive X-ray spectroscopy (EDS, Oxford) and high-resolution TEM (HRTEM). The UV-visible diffuse reflectance absorb feature of the NCPTNs was investigated on a UV-visible spectrophotometer (Cary 500 Scan Spectrophotometers, Varian, USA). $BaSO_4$ was used as a reflectance standard. X-ray photoelectron spectra for the NCPTNs were recorded on a Thermo ESCALAB 250Xi XPS. Electron spin resonance (ESR) spectra were recorded on JES FA200, X-band at room temperature. BET surface area was tested on BELSORP-mini surface area analyzer (BELSORP Co., Japan) using N_2 adsorption at 77 K.

2.3 Photocatalytic activity

The photocatalytic activities of the NCPTNs were evaluated by the decomposition of methylene blue (MB) (2×10^{-5} mol/L) in an aqueous solution. Visible light

photocatalytic reactions were performed in a 100 ml Pyrex glass vessel containing 80 mL MB aqueous solution and 80 mg catalyst. A 300 W halogen lamp (Philips Electronics) was used as a light source with two cutoff filters for ensuring the visible light irradiation between 420 nm and 850 nm during the photoreaction process. The photocatalysts were suspended in an aqueous solution and stirred for 1 h before irradiation to reach the adsorption/desorption equilibrium. A 4 ml aliquot was taken at 15 min intervals and then centrifuged. The resulting solution was analyzed on a Shimadzu UV-1750 UV-Vis-NIR spectrophotometer at wavelength 664 nm. The percentage of degradation is reported as $(C_0-C_t)/C_0$. In which, C_t is the concentration of MB at each irradiated time t min, while C_0 represents the starting concentration of MB at the adsorption/desorption equilibrium.

3. Results and discussion

3.1 XRD, SEM and TEM

Fig.1 shows the XRD patterns for the NCPTN-0 and the NCPTN-5 nanofibers. As shown in Fig.1, the diffraction peaks at *circa* 25.4°, 37.9°, 48.0°, 54.9° and 62.8° are assigned to the (101), (004), (200), (211) and (112) crystal planes of anatase type structure (PDF#21-1272), respectively. The results agreed well with the previous report that anatase TiO_2 crystallized at the temperature above 400℃,[27] suggesting that the decomposition of PVP at 400℃ gives no influence on the crystal structure of TiO_2. Moreover, the NCPTN-0 and NCPTN-5 nanofibers giving a similar curve in XRD pattern indicates that the introduction of 5 wt% urea leads to little change in the anatase phase.

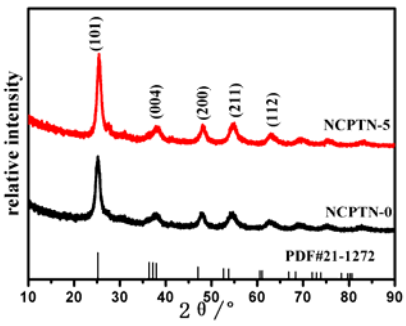

Fig.1 XRD patterns of NCPTN-0 and NCPTN-5.

The SEM and TEM experiments on PVP/$Ti(OiPr)_4$ and PVP/$Ti(OiPr)_4$/5wt％urea composite fibers before and after calcination are performed, respectively. The SEM images shown in Fig S1 reveal that all as-spun fibers have a smooth surface. The FESEM images of the NCPTN-0 and the NCPTN-5 fibers are shown in Fig.2. It is clear that the diameters of the two fibers are estimated to be 50-120 nm, and the introduction of urea as an additional nitrogen source changes the shape and the diameter of fibers with little.

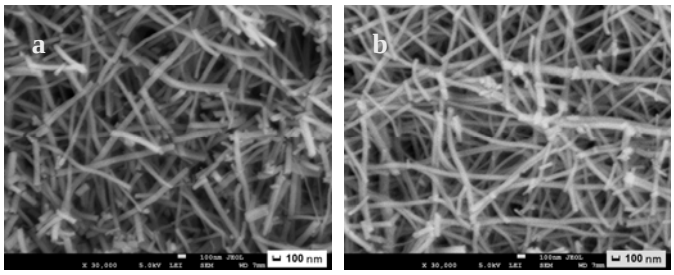

Fig.2 FESEM images of the NCPTN-0 (a) and the NCPTN-5 (b).

The morphology of the NCPTN-5 was also observed on TEM and HRTEM, respectively and the results are given in Fig.3. As shown in Fig.3, the prepared nanofibers are consisted of many polycrystalline nanograins with particle diameter ranging from 10 nm to 20 nm (Fig.3a). The grains are consisted of TiO_2 nanoparticles decorated with carbon (Fig.3b). The carbon residues are formed by partial decomposition of PVP and $Ti(OiPr)_4$. It is interested that some pores are found in the NCPTN-5 (Fig.3b and c). EDS analyses (Fig.3e-h) reveal that Ti, O, C, and N elements are detected in the prepared composite nanofibers, suggesting that the materials are N and C co-doped TiO_2 nanofibers.

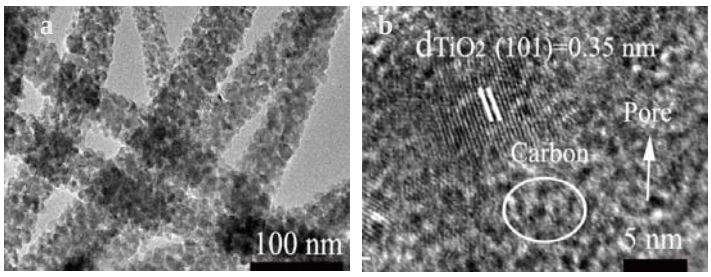

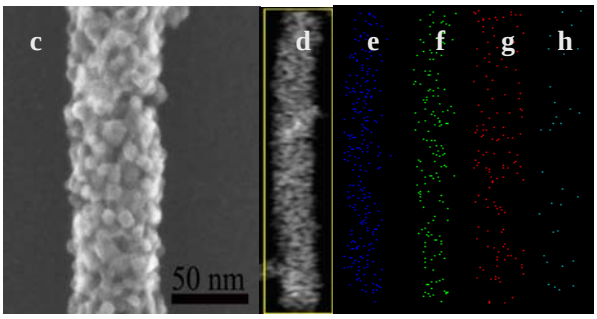

Element	Atomic%
Ti	11.32
O	34.45
C	51.73
N	2.50

Fig. 3 TEM(a), HRTEM(b), SEI-TEM(c), dark-field TEM(d) images and its corresponding EDS mapping for Ti, O, C, and N (e-h) of the NCPTN-5.

3.2 XPS

The N 1s, O 1s，C 1s and Ti 2p XPS spectra for NCPTN-0 and NCPTN-5 are shown in Figure 4. In the N 1s spectra for NCPTN-0, the N 1s peak at ~399 eV is assigned to the anionic N^- in the N-Ti-O linkages,[28,29] which is attributed to the occupied interstitial site in the TiO_2 lattices. No peaks are found at ～396 eV, indicating that no Ti-N bond formed in NCPTN-0.

The atomic percentages of nitrogen in the NCPTN-0 were determined to be 0.46 at.％ (Table S1). This suggests the decomposition of PVP is not complete at 400 ℃ for 1 h. Parts of N atoms derived from pyrrolidone units are incorporated into TiO_2 matrix. The atomic percentages of nitrogen only increase slightly to 0.48 at.％ by increase urea dosage to 5 wt%, suggesting that nitrogen are derived mainly from PVP rather than from urea. The N content of NCPTN-5 calculated from the XPS data is slightly lower than that obtained for EDS analysis. For XPS is a measurement technique mainly for surface characterization.

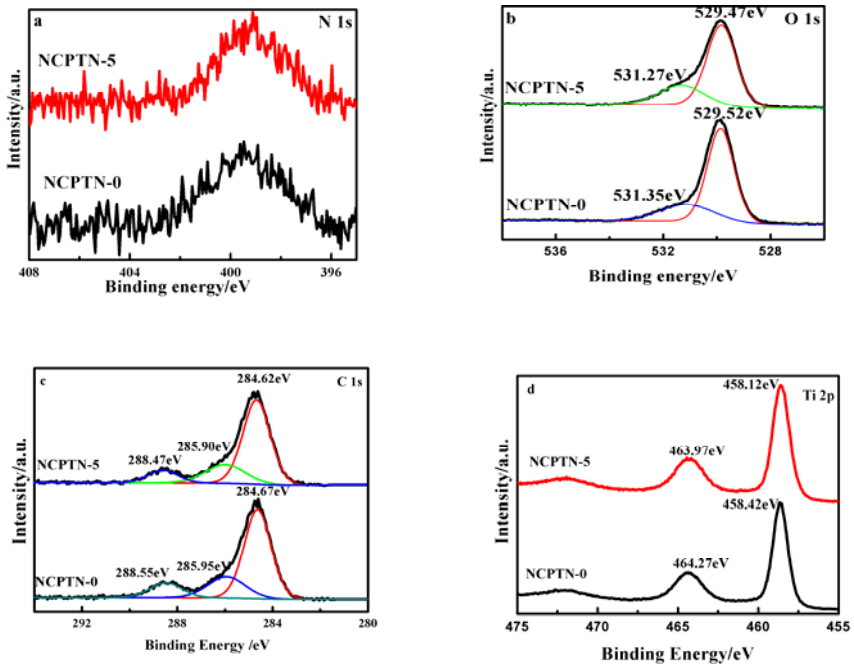

Fig.4 N 1s (a), O 1s (b), C 1s(c) and Ti 2p (d) XPS spectra for NCPTN-0 and NCPTN-5.

For C 1s spectrum of NCPTN-0 (Fig.4c), three peaks at about 284.67 eV, 285.95 eV and 288.55 eV are observed. The strongest peak at 284.67 eV is attributed to hydrocarbons from the internal standard carbon, while two peaks 285.95 eV and 288.55 eV are corresponded to the C-O and C=O bonds, respectively.[30] The results show the presence of carboxyl and carbonate species in NCPTN-0. The two carbon species are formed from the partial decomposition of PVP at 400 ℃. According to the previous literatures, [8,31,32] three forms of carbon species have been detected in C-doped TiO_2: elemental carbon located within the tetrahedral and octahedral interstices in the anatase crystal, the carbonate species adsorbed on the surface and carbon atoms substituting atoms in the lattice of TiO_2. In Fig.4c, no peak appears at 281 eV, indicating that no oxygen atom is substituted by carbon to form the Ti-C bond in the anatase lattice. Wu *et al.* suggested that the residual carbon chain of PVP did not decompose completely at temperatures less than 550℃ in the process of calcining PVP/SnO_2 nanofibers.[26]

Moreover, NCPTN-5 and NCPTN-0 give similar N 1s and C 1s curves, indicating that both urea and PVP can play roles as N and C sources for doping N and C onto the

resultant materials. Very little change is observed in the N 1s and C 1s spectra between NCPTN-0 and NCPTN-5. However, the O 1s and Ti 2p spectra of NCPTN-5 show relatively lower binding energy than those of NCPTN-0.

Ti 2p spectrum is given in Figure 4d. In Ti $2p_{3/2}$ region, the peak at 458.42 eV for NCPTN-0 and 458.12 eV for NCPTN-5 is lower than the typical binding energy of 458.8-458.9 eV in Ti $2p_{3/2}$ for TiO_2, [32,33] indicating the different electronic interactions of Ti with anions. It has been suggested that incorporation of carbon or nitrogen can lead to the formation of oxygen vacancies and result in a slight shift of the Ti 2p peaks toward the lower binding energy.[32] In our experiment, nitrogen is introduced into TiO_2 matrix by the decomposition of both PVP and urea, while carbon is doped by the adsorption of carbon species (mainly from the decomposition of PVP and $Ti(OiPr)_4$) on the surface of TiO_2.

The curves fitting for O 1s spectra were performed and the results are given in Fig.4b. For O 1s spectrum (Fig.4b), two peaks appeared at ~529 eV and ~531eV are attributed to Ti-O and chemisorbed oxygen from any of the species such as O^-, O^{2-} ions in the oxygen deficient regions on the surface,[29,34] respectively. Due to the fact that TiO_2 possess typical oxygen related defects, the defect sites are subject to the chemisorption of the above ions while sharing the lattice electrons. The area of the peak at ～531eV for NCPTN-5 is 1.1 times higher than that of NCPTN-0, confirming that a larger fraction of oxygen-defect regions is present in the surface layer for NCPTN-5 compared to NCPTN-0.

Furthermore, the ESR spectra (Fig.5) for NCPTN-0 and NCPTN-5 give a single ESR signal with g=2.0001, which is the characteristic ESR signal of single-electron-trapped oxygen vacancy (SETOV). Livraghi[35], Wang[36] and Sano[37] have proposed that the absorption features displayed in the visible spectral region are likely the result of formations of SETOV in the reduction of TiO_2. Serpone *et al.* also ascribed the origin of visible light absorption of N-doped TiO_2 to the formation of SETOV, and believed that the SETOV are more easily formed due to the partial reduction of TiO_2 during the doping process.[38] The intensity of the peak (g=2.0001) of NCPTN-5 is higher than that of NCPTN-0 due to the presence of urea in the former

precursor. It is well known that urea starts to decompose into ammonia and isocyanic acid at 300-420 ℃.[39] The reducibility of ammonia results in a large amount of SETOV in TiO_2 matrix of NCPTN-5 and NCPTN-10.

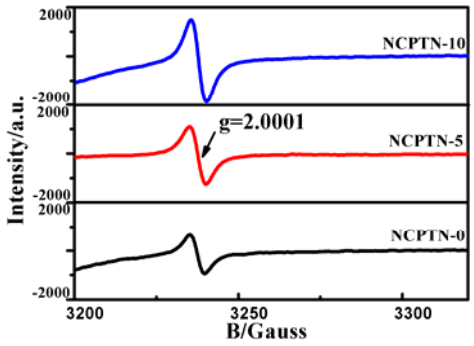

Fig.5 The ESR spectra for NCPTN-0, NCPTN-5 and NCPTN-10.

3.3 DRS

The diffuse reflectance spectra for NCPTN-0 and NCPTN-5 fibers are shown in Fig.6.

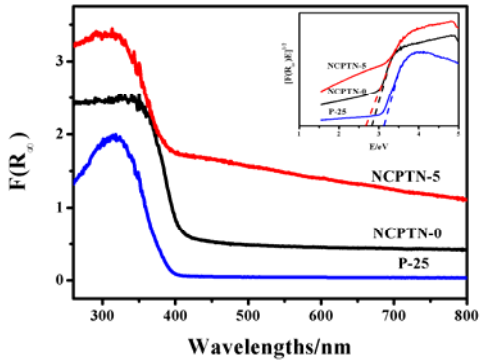

Fig.6 The diffuse reflectance spectra for P25, NCPTN-0 and NCPTN-5.

Both NCPTN-0 and NCPTN-5 exhibit absorption in the visible light region. NCPTN-0 gives an absorption edge of ~430 nm, while NCPTN-5 gives the one with a little broad edge of ~455 nm. The absorption intensities of NCPTN-0 in the visible light region are higher than that of P25, due to the synergetic effects of nitrogen and carbon doping. The significant difference is observed at the range of 400~800 nm. In this range, NCPTN-5 shows a notably higher photo absorption than NCPTN-0. More SETOV in contribute to the better absorption of TiO_2 in the visible spectral region.[35] Moreover, the incorporated nitrogen introduces a broad N 2p band, which leads to

decreasing band gap and enhancing the absorption at the longer wavelengths.[40] The band gap energy can be obtained from the plots of $[F(R_\infty)hv]^{1/2}$ *versus* the photo energy hv,[41] as presented in the inset of Fig.6. The Egs of both samples are 2.72 eV and 2.88 eV, respectively. The band gaps of both samples are slightly smaller than that of anatase TiO_2 (3.12 eV). This narrowed band-gap can be reasonably attributed to the location of N_{2p} band formed by interstitial N above the O 2p valence band,[42,43] demonstrating that the interstitial N species incorporated into the NCPTNs can enhance the visible light absorption and photocatalytic activity.

3.4 Photocatalytic activity

The photocatalytic activity of the prepared samples was evaluated using methylene blue as a model toxic organic compound under visible light irradiation. It is true methylene blue is an absorbing degradation substrate, and the degradation rate in the absence of catalyst was 18%. For comparison, the commercial titania, P-25, was also investigated. The results are shown in Fig.7.

As shown in Fig.7a, P-25 shows very low photocatalytic activity in visible light region. Under the irradiation of visible light for 120 min, the degradation rate of MB catalyzed by P-25 is lower than 20%, which is closed to that by no catalyst. However, the degradation rate of MB by with the presence of NCPTN-0 and NCPTN-5 increases to 47.3% and 95.0% respectively, suggesting that the prepared NCPTNs have high photocatalytic activity under visible light for MB degradation.

The effect of the urea concentration on the photocatalytic activity is given in Fig.7b. The degradation rate of MB increases from 47.3% to 81.5% and 95.0 % with raising the urea concentration from 1 wt% to 3 wt% and 5 wt%, indicating that using urea can obviously improve the photo degradation efficiency of the TiO_2 nanofibers. Whereas the degradation rate of MB decreases to 70.9% and 65.3% by further increasing the concentration to 10 wt% and 20 wt%, indicating that an excess of nitrogen and carbon may provide possibly the recombination sites of electrons and holes, thus reducing the photocatalytic activity.[8] It is worth noting that the surface area of NCPTN-10 is 100.58 m^2/g lower than that of NCPTN-5 (114.41 m^2/g), and the absorption intensities of NCPTN-10 in the visible light region are also lower than that

of NCPTN-5 (Table S2 and Fig. S2).

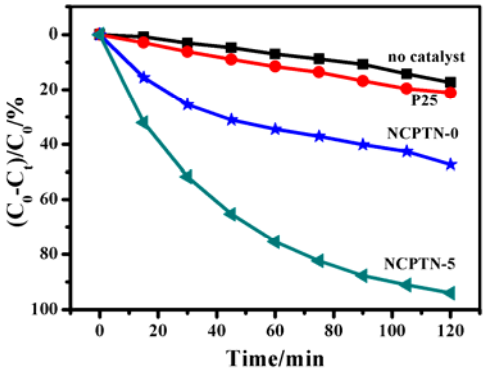

Fig.7a

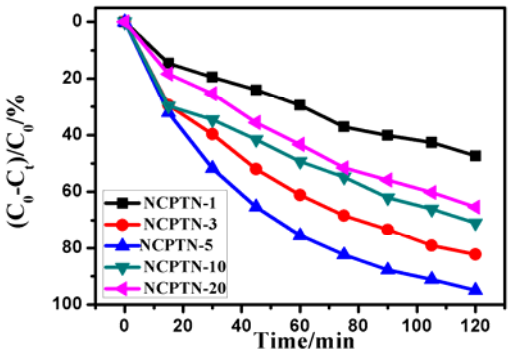

Fig.7b

Fig.7 The photocatalytic degradation of MB on (a) various catalysts, (b) catalysts obtained from various urea dosages.

Based on the previous results, the photocatalytic mechanism for the prepared NCPTNs can be proposed in Scheme 1.

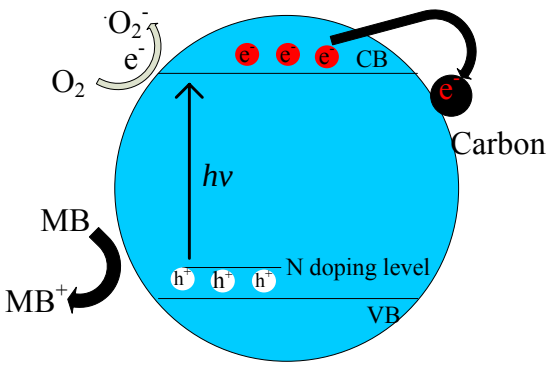

Scheme 1 The proposed photocatalytic mechanism over the NCPTNs

We suggest that there was a synergistic effect of the heterogeneous structure of the NCPTNs on the MB degradation. Firstly，it is widely accepted that the doped N

species located at the interstitial sites in TiO_2 lead to the band gap narrowing of TiO_2.[42] In XPS spectra of N 1s (Fig.4a), both NCPTN-0 and NCPTN-5 gives a binding energy of ca. 399 eV, suggesting the formation of N-Ti-O bonds in the TiO_2 matrix.[44] Moreover, the energy gap (2.88 eV) of NCPTN-0 is lower than the typical value (3.12 eV) of anatase, revealing that an N-doping level above the O 2p valance band is formed. Firstly, the electrons are excited from the nitrogen surface species to the conduction band of the TiO_2 matrix under visible light irradiation. The photogenerated electrons then are directly captured by the O_2 molecules adsorbed on the surface of NCPTNs to form O_2^-, which is capable of degrading MB. Compared with NCPTN-0, NCPTN-5 has a lower energy gap of 2.72 eV and shows higher photocatalytic activity in wider light spectra due to its larger amount of SETOV. The reducibility of ammonia derived from the decomposition of urea at 300-420ºC leads to the enhancement of the SETOV in NCPTN-5.[45] Wang has proposed that the enhanced visible light photoabsorption of N-doped TiO_2 sample is proportional to the concentration of SETOV.[36,46,47] Furthermore, the carbonaceous species on the surface of NCPTNs, derived from the thermal decomposition of PVP by calcination, can cause reduced reflection of light. This reveals that the doped carbon species on NCPTN may be another important factor for the photocatalytic activity. Koichi[48], Timothy[8], Maria[49] *et al.* also have suggested that the carbons can absorb the electrons and promote the separation of the electrons and holes to maintain their high reactivity. However, the oxygen vacancies also acted as recombination centers for holes and electrons.[50] In calcination process, higher concentration of urea causes to form larger number of SETOV and more residue on the surface of TiO_2, resulting in the decrement of the surface area.

The adsorption capacity is also an efficient factor to effluent the photocatalytic property of a catalyst for degradation of an organic compound.[51] High surface area results in a high adsorption capacity for MB in the aqueous solution. Xu *et al.* have proposed that the abundant adsorption of MB molecules on the surfaces of catalysts can shorten the diffusion distances and facilitate the mass transfer of reactant molecules from the solution to active sites on TiO_2.[52] NCPTN-5 possesses higher BET

surface area (114.41 m^2/g) than NCPTN-0 (83.19 m^2/g) (Table S2) and shows higher photocatalytic activity.

4. Conclusion

In this study, the nitrogen and carbon co-doped porous TiO_2 nanofibers (NCPTNs) were developed by a combination of electrospinning and calcinations technologies. The nitrogen atoms found to be incorporated into the anatase lattice, while a carbonaceous layer was introduced on the surface of TiO_2 matrix. The co-doping of nitrogen and carbon onto TiO_2 not only leads to a shift of the absorption edge to low energy by inducing new band levels, but also creates large amounts of single-electron-trapped oxygen vacancy. The porosity of the prepared materials provides large active points for the photo-decomposition reaction of methylene blue. The N-C co-doped porous TiO_2 obtained with the presence of 5 wt% urea shows the highest photocatalytic activity.

Acknowledgments

This work was supported by National Natural Science Foundation of China (21307012), Natural Science Foundation of Fujian Province, China(Grant No.2014J01036)，and Educational Commission of Fujian Province (JK2013007, JA13086).

Reference

1. X. Chen and S. S. Mao, *Chemical Reviews*, 2007, 107, 2891-2959.
2. J. H. Pan, Z. Cai, Y. Yu and X. S. Zhao, *Journal of Materials Chemistry*, 2011, 21, 11430-11438.
3. K. H. A. Fujishima, *Nature*, 1972, 238, 37-38.
4. Z. Cai, J. Teng, Z. Xiong, Y. Li, Q. Li, X. Lu and X. S. Zhao, *Langmuir*, 2011, 27, 5157-5164.
5. Z. Cai, Z. Xiong, X. Lu and J. Teng, *Journal of Materials Chemistry A*, 2014, 2, 545-553.
6. D. Chen, Z. Jiang, J. Geng, Q. Wang and D. Yang, *Industrial & Engineering Chemistry Research*, 2007, 46, 2741-2746.
7. D. Fattakhova-Rohlfing, A. Zaleska and T. Bein, *Chemical Reviews*, 2014, 114, 9487-9558.
8. Q. C. Xu, D. V. Wellia, S. Yan, D. W. Liao, T. M. Lim and T. T. Y. Tan, *Journal of Hazardous Materials*, 2011, 188, 172-180.
9. D. Li, H. Haneda, S. Hishita and N. Ohashi, *Chem Mater*, 2005, 17, 2588-2595.
10. D. Li, H. Haneda, S. Hishita and N. Ohashi, *Chem Mater*, 2005, 17, 2596-2602.
11. K.-R. Wu and C.-H. Hung, *Appl. Surf. Sci.*, 2009, 256, 1595-1603.

12. Y. Cong, F. Chen, J. Zhang and M. Anpo, *Chemistry Letters*, 2006, 35, 800-801.
13. T. Sano, N. Negishi, K. Koike, K. Takeuchi and S. Matsuzawa, *Journal of Materials Chemistry*, 2004, 14, 380-384.
14. D. Noguchi, Y. Kawamata and T. Nagatomo, *Journal of The Electrochemical Society*, 2005, 152, D124-D129.
15. M. Kapilashrami, Y. Zhang, Y.-S. Liu, A. Hagfeldt and J. Guo, *Chemical Reviews*, 2014, 114, 9662-9707.
16. J. Li, H. Qiao, Y. Du, C. Chen, X. Li, J. Cui, D. Kumar and Q. Wei, *The Scientific World Journal*, 2012, 2012, 154939.
17. V. J. Babu, M. K. Kumar, A. S. Nair, T. L. Kheng, S. I. Allakhverdiev and S. Ramakrishna, *International Journal of Hydrogen Energy*, 2012, 37, 8897-8904.
18. L. Lang, D. Wu and Z. Xu, *Chemistry – A European Journal*, 2012, 18, 10661-10668.
19. A. Mezzi, S. Kaciulis, I. Cacciotti, A. Bianco, G. Gusmano, F. R. Lamastra and M. E. Fragalà, *Surface and Interface Analysis*, 2010, 42, 572-575.
20. C. Graf, D. L. J. Vossen, A. Imhof and A. van Blaaderen, *Langmuir*, 2003, 19, 6693-6700.
21. J.-G. Kim, D. Shi, K.-J. Kong, Y.-U. Heo, J. H. Kim, M. R. Jo, Y. C. Lee, Y.-M. Kang and S. X. Dou, *ACS Applied Materials & Interfaces*, 2013, 5, 691-696.
22. D. Li and Y. Xia, *Nano Letters*, 2003, 3, 555-560.
23. J. A. Lee, K. C. Krogman, M. Ma, R. M. Hill, P. T. Hammond and G. C. Rutledge, *Advanced Materials*, 2009, 21, 1252-1256.
24. C. Peniche, D. Zaldívar, M. Pazos, S. Páz, A. Bulay and J. S. Román, *J. Appl. Polym. Sci.*, 1993, 50, 485-493.
25. Y. Borodko, S. M. Humphrey, T. D. Tilley, H. Frei and G. A. Somorjai, *The Journal of Physical Chemistry C*, 2007, 111, 6288-6295.
26. J. Wu, D. Zeng, X. Wang, L. Zeng, Q. Huang, G. Tang and C. Xie, *Langmuir*, 2014, 30, 11183-11189.
27. S. Chuangchote, J. Jitputti, T. Sagawa and S. Yoshikawa, *ACS Applied Materials & Interfaces*, 2009, 1, 1140-1143.
28. M. Sathish, B. Viswanathan, R. P. Viswanath and C. S. Gopinath, *Chem Mater*, 2005, 17, 6349-6353.
29. V. J. Babu, R. P. Rao, A. S. Nair and S. Ramakrishna, *Journal of Applied Physics*, 2011, 110, 064327.
30. B. Zhao, R. Cai, S. Jiang, Y. Sha and Z. Shao, *Electrochimica Acta*, 2012, 85, 636-643.
31. X. Wang, S. Meng, X. Zhang, H. Wang, W. Zhong and Q. Du, *Chemical Physics Letters*, 2007, 444, 292-296.
32. Y.-F. Lee, K.-H. Chang, C.-C. Hu and K.-M. Lin, *Journal of Materials Chemistry*, 2010, 20, 5682-5688.
33. E. M. Rockafellow, X. Fang, B. G. Trewyn, K. Schmidt-Rohr and W. S. Jenks, *Chem Mater*, 2009, 21, 1187-1197.
34. F. Kayaci, S. Vempati, I. Donmez, N. Biyikli and T. Uyar, *Nanoscale*, 2014, 6, 10224-10234.
35. S. Livraghi, M. R. Chierotti, E. Giamello, G. Magnacca, M. C. Paganini, G. Cappelletti and C. L. Bianchi, *The Journal of Physical Chemistry C*, 2008, 112, 17244-17252.
36. Y. Wang, C. Feng, M. Zhang, J. Yang and Z. Zhang, *Applied Catalysis B: Environmental*, 2010, 100, 84-90.

37. T. Sano, N. Mera, Y. Kanai, C. Nishimoto, S. Tsutsui, T. Hirakawa and N. Negishi, *Applied Catalysis B: Environmental*, 2012, 128, 77-83.
38. N. Serpone, *The Journal of Physical Chemistry B*, 2006, 110, 24287-24293.
39. D. Mitoraj and H. Kisch, *Angewandte Chemie International Edition*, 2008, 47, 9975-9978.
40. T. M. Breault and B. M. Bartlett, *The Journal of Physical Chemistry C*, 2012, 116, 5986-5994.
41. R. Beranek and H. Kisch, *Photochemical & Photobiological Sciences*, 2008, 7, 40-48.
42. J. Fang, F. Wang, K. Qian, H. Bao, Z. Jiang and W. Huang, *The Journal of Physical Chemistry C*, 2008, 112, 18150-18156.
43. R. Asahi, T. Morikawa, T. Ohwaki, K. Aoki and Y. Taga, *Science*, 2001, 293, 269-271.
44. Z. Xiong and X. S. Zhao, *Journal of the American Chemical Society*, 2012, 134, 5754-5757.
45. C. Feng, Y. Wang, Z. Jin, J. Zhang, S. Zhang, Z. Wu and Z. Zhang, *New Journal of Chemistry*, 2008, 32, 1038-1047.
46. X. Wang and T.-T. Lim, *Applied Catalysis B: Environmental*, 2010, 100, 355-364.
47. Y. Wang, M. Jing, M. Zhang and J. Yang, *Catalysis Communications*, 2012, 20, 46-50.
48. H. Kamisaka, T. Adachi and K. Yamashita, *The Journal of Chemical Physics*, 2005, 123, 084704.
49. L. Zhao, X. Chen, X. Wang, Y. Zhang, W. Wei, Y. Sun, M. Antonietti and M.-M. Titirici, *Advanced Materials*, 2010, 22, 3317-3321.
50. H. Irie, Y. Watanabe and K. Hashimoto, *The Journal of Physical Chemistry B*, 2003, 107, 5483-5486.
51. D. Teng, Y. Yu, H. Liu, X. Yang, S. Ryu and Y. Lin, *Catalysis Communications*, 2009, 10, 442-446.
52. D.H. Wang, L. Jia, X.L. Wu, L.Q. Lu and A.W. Xu, *Nanoscale*, 2012, 4, 576-584.